ISBN: 978-3-95450-214-1 ISSN: 2673-5490 doi:10.18429/JACoW-IPAC2021-MOPAB032

ESTIMATES OF COLLECTIVE EFFECTS FOR FCC-e^+e^- PRE-BOOSTER RING

O. Etisken*, Y. Papaphilippou, F. Antoniou, F. Zimmermann, K. Oide[1], CERN, Geneva, Switzerland
A. K. Ciftci, Izmir University of Economics, Izmir, Turkey
[1]also at KEK, Tsukuba, Ibaraki, Japan

Abstract

The FCC-e^+e^- injector complex needs to produce and to transport high intensity e^+ and e^- beams at a fast repetition rate for topping up the collider at its collision energy. Two different options are under consideration as pre-accelerator before the bunches are transferred to the high-energy booster: either using the existing SPS machine or designing a completely new ring. The purpose of this paper is to present the studies of collective effects with analytical estimates for both the pre-booster ring design options including space charge (SC), longitudinal micro-wave instability (LMI), transverse mode coupling instability (TMCI), ion effects, electron cloud (e-cloud), coherent synchrotron radiation (CSR) and intra-beam scattering (IBS).

INTRODUCTION

The Future Circular Collider (FCC) e^+e^- project is a design study of a high-luminosity, high-energy circular electron-positron collider to be installed in a new tunnel of around 100 km circumference. It is planned to be used as a high precision machine for the investigation of the Z, W, Higgs and top particles at center of mass energies varying between 91.2 and 365 GeV [1, 2].

The injector complex design of the FCC-e^+e^- consists of an e^+/e^- linac, which accelerates the beams up to 6 GeV, a pre-booster ring (PBR), accelerating the beams from 6 GeV to 16 GeV, and a booster synchrotron ring (BR) integrated in the collider tunnel, accelerating the beams up to the collision energy [3]. The existing SPS with some modifications is considered as the baseline for the PBR. In addition, an alternative PBR design was also studied for the injector complex [4]. The beam parameters for the PBR options are summarized in Table 1.

Collective effects can be a bottle-neck in the performance of an accelerator, limiting its ultimate reach. In this study, analytical estimates related to collective effects have been performed for the two PBR options.

COLLECTIVE EFFECT ESTIMATES

Space Charge

The incoherent tune spread caused by the Space Charge (SC) effect can lead to the interaction of the beam with resonances and consequently to beam degradation [5–7]. An analytical expression for the incoherent SC tune shift for Gaussian bunches is given by [8–10]:

$$\delta Q_y^{\mathrm{inc}} = -\frac{N_b r_e C}{(2\pi)^{\frac{3}{2}}\beta^2\gamma^3\sigma_z\sqrt{\epsilon_y}}\left\langle \frac{\sqrt{\beta_y}}{\sqrt{\beta_x\epsilon_x + D_x^2\sigma_\delta^2}+\sqrt{\epsilon_y\beta_y}}\right\rangle, \tag{1}$$

where r_e is the electron radius, C the circumference and N_b the bunch population, ϵ_x and ϵ_y the geometrical transverse emittances, D_x the horizontal dispersion and $\beta_{x,y}$ the horizontal and vertical betatron functions, respectively.

For flat beams, i.e. when the vertical emittance is much smaller than the horizontal one, the vertical tune spread is higher and therefore more critical. For the case of the PBR, the maximum value is computed at the end of the injection plateau, after the beam reaches the equilibrium emittance values in all planes. For the case of the alternative PBR design $\delta Q_y^{\mathrm{inc}} = -0.028$ while for the case of the SPS $\delta Q_y^{\mathrm{inc}} = -0.018$. For both cases, the values are small and thus the SC is not expected to pose a limitation with respect to transverse emittance blow up or particle losses.

Intra-Beam Scattering

Intra-beam Scattering (IBS) refers to the binary Coulomb scattering events between the particles within a beam, leading to the re-distribution of the phase space. Above transition, IBS can lead to emittance blow-up in all three planes [5, 11, 12]. Figure 1 shows the horizontal emittance evolution during the injection plateau, with (dashed lines) and without (solid lines) taking into account the IBS effect. The results for the alternative PBR design are shown in red,

Table 1: Beam Parameters of the PBR Options

Parameter	SPS	Alt. PBR
Energy, E [GeV]	6/16	6/16
Circumference, C [m]	6911.5	2030.4
Geo. emit. (h), ϵ_x [nm·rad]	0.9/5.6	0.66/4.74
Bunch length, σ_z [mm]	41/55	5.9/7.2
Momentum sprd., σ_δ ($\times10^{-2}$)	0.3/0.38	0.03/0.1
Harmonic number, h	9215	2706
Mom. compac., α_c ($\times10^{-3}$)	0.98	0.32
Horizontal tune, Q_h	40.35	63.68
Vertical tune, Q_v	26.72	27.19
Synchrotron tune, Q_s	0.08/0.05	0.007/0.01
Energy loss/turn, U_0 [MeV]	3.4/31.5	0.57/29.2
Chamber radius, b [m]	0.04	0.03
Bunch pop., N_b ($\times10^{10}$)	2.13	2.13
Bunch spacing, ΔT_b [ns]	15-20	20
Number of bunches, n_b	1190	320

* ozgur.etisken@cern.ch

ISBN: 978-3-95450-214-1 ISSN: 2673-5490 doi:10.18429/JACoW-IPAC2021-MOPAB032

while for the SPS design in blue. The calculations were done using the IBS module of MAD-X [13]. The emittance growth with respect to the natural equilibrium emittance (without IBS) at the end of the injection plateau is around 6% for the alternative design and 9% for the SPS design. The effect is much smaller at the extraction energy. Consequently, the IBS effect is not expected to pose a limitation for both PBR options.

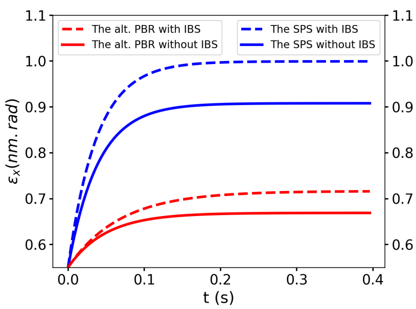

Figure 1: Emittance (hor.) evolution on the injection plateau of the SPS (blue) and the alternative PBR design (red).

Longitudinal Microwave Instability

A broad-band impedance, representing the effect of all discontinuities of the beam pipe, can cause a microwave instability. According to the Boussard criterion, the corresponding threshold impedance is given by [8, 14]:

$$\frac{Z_0^{\parallel}}{n} = Z_0 \frac{\pi}{2} \frac{\gamma \alpha_c \sigma_\delta{}^2 \sigma_z}{N_b r_e} \left(\frac{b}{\sigma_z}\right)^2, \quad (2)$$

where Z_0 is the impedance of free space. Based on the PBR design parameters for both options, the Boussard threshold impedance $Z_0{}^{\parallel}/n$ was calculated at injection, at the end of the injection plateau and at extraction. The results are summarized in Table 2. For the case of the alternative design they correspond to 57.9 Ω, 1.4 Ω and 10.1 Ω, while for the SPS design to 1167 Ω, 31.4 Ω, 100 Ω, respectively. The SPS longitudinal impedance is 6.4 Ω [15]. For the alternative PBR, a 1 Ω impedance is assumed, as the design of modern accelerators can easily allow for an impedance of that magnitude, or even lower. For both options, the longitudinal impedance is well below the threshold.

Transverse Mode Coupling Instability

The transverse impedance of the machine can drive the head-tail instability (HTI) and/or the transverse mode coupling instability (TMCI) [8]. The TMCI threshold for a broad-band resonator impedance is given by [8, 14]:

$$R_{\text{th}}[\text{k}\Omega/\text{m}] = \frac{0.6E[\text{GeV}]Q_s Q}{\beta_y[\text{m}]Q_b[\text{C}]\sigma_t[\text{ps}]f_r^2[\text{GHz}]}, \quad (3)$$

where $Q_b = N_b e$, $f_r = W_r/(2\pi)$, $W_r = c/b$, $\sigma_t = \sigma_z/c$. The thresholds for both designs were estimated at injection, at the end of the injection plateau and at extraction and correspond to 5.3 MΩ/m, 8.9 MΩ/m and 37.0 MΩ/m for the alternative PBR and to 29.6 MΩ/m, 7.1 MΩ/m and 9 MΩ/m for the SPS. The transverse impedance is linked to the longitudinal impedance through [5, 9]:

$$Z_t{}^{\perp} = \frac{C}{\pi b^2} \frac{Z_0{}^{\parallel}}{n}. \quad (4)$$

Based on this, the transverse impedance ($Z_t{}^{\perp}$) of the alternative PBR is estimated as 0.8 MΩ/m, which is well below the calculated threshold. On the other hand, the transverse impedance for the case of the SPS is estimated at 9.8 MΩ/m, which is above the threshold computed at the end of the injection plateau and at extraction. The new necessary elements for the e^+/e^- option of the SPS (RF, transfer elements, vacuum etc.) needs to be designed taking into account not only these impedance considerations but also the thresholds allowing seamless proton beam operation.

Ion Effects

Ions can be created in the vacuum chamber from the interaction of charged particles in the beam with the residual gas in the beam pipe. These ions can be trapped and accumulated by the fields of the electron beam and eventually can lead to beam instability [16–18]. The critical mass for trapping of a singly charged ion is [8, 9]:

$$A_{\text{crit}} \cong \frac{N_b \Delta T_b c r_p}{2\sigma_y(\sigma_x + \sigma_y)}, \quad (5)$$

where r_p is the classical proton radius.

Figure 2 shows the critical mass computed for the alternative PBR (top) and the SPS (bottom) as well as the thresholds for different ions. The trapping condition is lower than almost all the possible ions' thresholds for both PBR options.

Ions trapped around the electron beam induce a tune shift, which at the end of the train is given by [8, 9, 16]:

$$\delta Q_{\text{ion}} \cong \frac{N_b n_b r_e c}{\pi \gamma \sqrt{\epsilon_x \epsilon_y}} \left(\frac{\sigma_{\text{ion}} p}{k_B T}\right), \quad (6)$$

where σ_{ion} is the ionization cross section, p is the vacuum pressure, k_B is the Boltzmann constant. For the alternative PBR $\delta Q_{\text{ion}} = 0.002$ while for the SPS $\delta Q_{\text{ion}} = 0.009$, which are both relatively small, assuming a pressure of 10^{-10} mbar for the alternative PBR and 10^{-11} mbar for the SPS, which may drive pumping upgrade considerations.

The accumulated ions can lead to the fast-ion instability (FII) with a rise time given by [8, 9, 16, 17]:

$$\tau_{\text{inst}} \cong \frac{0.1\gamma\sigma_x\sigma_y}{N_b n_b c r_e \beta_y \sigma_{\text{ion}}} \left(\frac{k_B T}{p}\right)\left(\sqrt{\frac{8}{\pi}}\right). \quad (7)$$

The FII rise times are obtained as 61 and 134 revolution times (t_{rev}) for the SPS and the alternative PBR, respectively. Instabilities with such rise times can be compensated with a feedback system, provided that 10^{-11} mbar SPS and 10^{-10} mbar alternative ring vacuum pressures are achieved.

ISBN: 978-3-95450-214-1 ISSN: 2673-5490 doi:10.18429/JACoW-IPAC2021-MOPAB032

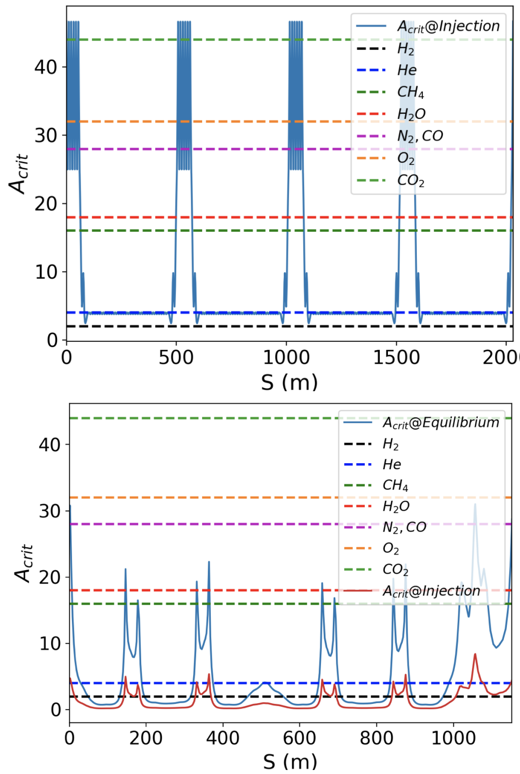

Figure 2: Critical mass for the alternative PBR (top) and one sextant of the SPS (bottom) in comparison to the thresholds for various molecules.

Electron Cloud

The e-cloud instability mostly arises for e^+ beams [17,19]. When free electrons in the vacuum chamber get accelerated in the electromagnetic field of the beam and hit the chamber walls, electron amplification can occur through the multi-pacting effect. The e^- build up saturates when the attractive beam field is compensated by the field of the electrons, at a neutralization density, given by [17]:

$$\rho_{\text{neutr}} = \frac{N_b}{L_{\text{sep}} \pi b_x b_y}, \quad (8)$$

where L_{sep} [m] is the bunch spacing. Electron cloud can lead to single or coupled-bunch instabilities. The single bunch e^-cloud instability (ECI) occurs above the e^- density threshold estimated by [17,20,21]:

$$\rho_{\text{th}} = \frac{2\gamma Q_s}{\sqrt{3} Q r_e \beta_y C}, \quad (9)$$

where $Q = \min(7, \frac{w_e \sigma_z}{c})$ is the angular oscillation frequency of the electrons interacting with the beam, with $w_e{}^2 = \frac{N_b r_e c^2}{2\sigma_z \sigma_y (\sigma_x + \sigma_y)}$. The neutralization densities for both the alternative PBR and the SPS options were calculated as $12.55 \times 10^{11}/\text{m}^3$ and $7.06 \times 10^{11}/\text{m}^3$, respectively. The neutralization density exceeds the threshold for both designs (see Table 2). This should be investigated with detailed simulations.

Table 2: Collective Effects Estimates for the PBR Options

Parameters	**SPS**	**Alt. PBR**
SC tune shift @inj.	0.0005	0.0032
SC tune shift @eq.	0.018	0.028
SC tune shift @ext. [$\times 10^{-4}$]	0.16	1.6
Emit. growth by IBS @inj. [%]	9	6
Longitudinal imp. [Ω]	6.44	1
LMI th. @inj. [Ω]	1167	57.92
LMI th. @eq. [Ω]	31.14	1.44
LMI th. @ext. [Ω]	100	10.11
Transverse impedance [MΩ/m]	9.77	0.79
TMCI th. @inj. [MΩ/m]	29.6	5.28
TMCI th. @eq. [MΩ/m]	7.10	8.95
TMCI th. @ext. [MΩ/m]	8.97	37.0
Chamber radius [m]	0.04	0.03
Max. tune shift by ions	0.009	0.002
FII rise time [t_{rev}]	61	134
e-cloud neutr. dens. [$10^{11}/\text{m}^3$]	7.06	12.55
ECI dens. th. @inj. [$10^{11}/\text{m}^3$]	11.30	2.84
ECI dens. th. @eq. [$10^{11}/\text{m}^3$]	1.62	1.43
ECI dens. th. @ext. [$10^{11}/\text{m}^3$]	1.68	3.67
$0.5\rho\Lambda^{-3/2}$ [cm]	5000	0.015
$\frac{\rho}{b}$	18525	6433
Stupakov parameter (Λ)	3.78	568

Coherent Synchrotron Radiation

Coherent synchrotron radiation (CSR) occurs if the SR wavelength is comparable to the bunch length. The CSR may lead to a micro-bunching instability under the following conditions [5,22–25]:

$$\sigma_z \geq 0.5\rho\Lambda^{-3/2} \qquad \text{and} \qquad \frac{\rho}{b} \leq \Lambda, \quad (10)$$

where b is the chamber radius, ρ the bending radius and Λ known as the Stupakov-Heifets parameter:

$$\Lambda = \frac{N_b r_e \rho \sqrt{2\pi}}{C|\alpha_c|\sigma_z \gamma \sigma_\delta{}^2}. \quad (11)$$

The instability conditions were calculated for both design options and presented in Table 2, showing that no CSR instability is expected.

CONCLUSION

In this study, analytical estimates of various collective effects were presented for the two FCC-e^+e^- PBR design options. Based on these, no major limitations are expected due to SC, IBS, LMI and CSR. Concerning the TMCI, the transverse impedance exceeds the instability threshold for the SPS. Furthermore, it was shown that the neutralization density exceeds the e-cloud instability threshold for both design options. The fast rise times of the FII can be compensated with a feedback system, provided a vacuum pressure of 10^{-11} mbar and 10^{-10} mbar are achieved for the SPS and the alternative design, respectively.

ISBN: 978-3-95450-214-1 ISSN: 2673-5490 doi:10.18429/JACoW-IPAC2021-MOPAB032

REFERENCES

[1] A. Abada *et al.*, "FCC-ee: The lepton collider", *Eur. Phys. J. Spec. Top.*, vol. 228, pp. 261–-623, 2019. doi:10.1140/epjst/e2019-900045-4

[2] K. Oide *et al.*, "Design of beam optics for the future circular collider e^+e^- rings", *Physical Review Accelerators and Beams*, vol. 19, p. 111005, 2016. doi:10.1103/PhysRevAccelBeams.19.111005

[3] S. Ogur *et al.*, "Overall injection strategy for FCC-ee", in *Proc. 62nd ICFA Advanced Beam Dynamics Workshop on High Luminosity Circular e^+e^- Colliders (eeFACT'18)*, Hong Kong, China, Sep. 2018, pp. 131–138. doi:10.18429/JACoW-eeFACT2018-TUPAB03

[4] O. Etisken, F. Antoniou, Y. Papaphilippou, T. Tydecks, and A. K. Çiftçi, "Updates on alternative pre-booster ring design and wiggler magnet considerations of SPS for the FCC e e injector", in *Proc. 10th Int. Particle Accelerator Conf. (IPAC'19)*, Melbourne, Australia, May 2019, pp. 1094–1097. doi:10.18429/JACoW-IPAC2019-MOPTS097

[5] A. Wolski, "Beam dynamics in high energy particle accelerators", London, UK: Imperial College Press, 2014.

[6] M. Ferrario, M. Migliorati, and L. Palumbo, "Space charge effects", in *Proc. of the CAS-CERN Accelerator School: Advanced Accelerator Physics*, , Trondheim, Norway, Aug. 2013, CERN-2014-009, pp. 331–356. doi:10.5170/CERN-2014-009.331

[7] W. T. Weng, "Space Charge Effects-Tune shifts and resonances", SLAC, Stanford, CA, USA, Rep. SLAC-PUB-4058, Aug. 1986.

[8] G. Rumolo, J. B. Jeanneret, Y. Papaphilippou, and D. Quatraro, "Collective Effects in the CLIC Damping Rings", in *Proc. 11th European Particle Accelerator Conf. (EPAC'08)*, Genoa, Italy, Jun. 2008, paper MOPP049, pp. 658–660.

[9] F. Zimmermann, T. A. Agoh, M. Korostelev, D. Schulte, and K. Yokoya, "Collective effects in the CLIC damping rings", in *Proc. 21st Particle Accelerator Conf. (PAC'05)*, Knoxville, TN, USA, May 2005, paper RPPP012, pp. 1312–1314.

[10] K. Schindl, "Space charge", in *Proc. of CAS - CERN Accelerator School: Basic Course on General Accelerator Physics*, Montreux, Switzerland, May 1998, pp. 305–320. doi:10.5170/CERN-2006-002.305

[11] H. Wiedemann, "Particle accelerator physics", Berlin Heidelberg: Springer, 2015.

[12] F. Antoniou, "Optics design of intrabeam scattering dominated damping rings", Ph.D. thesis, CLIC – Note – 989, CERN-THESIS-2012-368, National Technical University of Athens, Greece, 2013.

[13] CERN - BE/ABP Accelerator Beam Physics Group, "Methodical Accelerator Design", http://mad.web.cern.ch/mad/.

[14] E. Koukovini, K. S. B. Li, N. Mounet, G. Rumolo, and B. Salvant, "Impedance effects in the CLIC damping rings", in *Proc. 2nd Int. Particle Accelerator Conf. (IPAC'11)*, San Sebastian, Spain, Sep. 2011, paper TUPC050, pp. 1111–1113.

[15] D. Brandt *et al.*, "Beam dynamics effects in the CERN SPS used as a lepton accelerator", in *Proc. 13th Particle Accelerator Conf. (PAC'89)*, Chicago, IL, USA, Mar. 1989, pp. 1205–1208.

[16] F. Zimmermann, *et al.* "Experiments on the fast beam-ion instability at the ALS", SLAC, Stanford, CA, USA, Rep. SLAC-PUB-7617, Oct. 1997.

[17] F. Zimmermann, "Two-stream effects in present and future accelerators", in *Proc. 8th European Particle Accelerator Conf. (EPAC'02)*, Paris, France, Jun. 2002, paper THZGB001, pp. 25–29.

[18] R. Nagaoka, "Ions", *in Proc. CAS-CERN Accelerator School: Intensity Limitations in Particle Beams*, CERN-2017-006-SP, CERN, Geneva, Switzerland, Nov. 2015, vol. 3, pp. 519–556. doi:10.23730/CYRSP-2017-003.519

[19] G. Rumolo and G. Iadarola, "Electron clouds", in *Proc. CAS-CERN Accelerator School: Intensity Limitations in Particle Beams*, CERN, Geneva, Switzerland, Nov. 2015, pp. 411-430. doi:10.23730/CYRSP-2017-003

[20] E. Belli, P. Costa Pinto, G. Rumolo, T. F. Sinkovits, M. Taborelli, and M. Migliorati, "Electron cloud studies in FCC-ee", in *Proc. 9th Int. Particle Accelerator Conf. (IPAC'18)*, Vancouver, Canada, Apr.-May 2018, pp. 374–377. doi:10.18429/JACoW-IPAC2018-MOPMK012

[21] K. Ohmi, S. Heifets, and F. Zimmermann, "Study of coherent tune shift caused by electron cloud in positron storage rings", in *Proc. 2nd Asian Particle Accelerator Conf. (APAC'01)*, Beijing, China, Sep. 2001, paper WEP056, pp. 529–531.

[22] G. Stupakov and S. Heifets. "Beam instability and microbunching due to coherent synchrotron radiation", *Physical Review Special Topics-Accelerators and Beams*, vol. 5, p. 054402, 2002.

[23] G. Stupakov and S. Heifets. "Beam instability and microbunching due to coherent synchrotron radiation", SLAC, Stanford, CA, USA, Rep. SLAC-PUB-8761, Feb. 2001.

[24] C.-Y. Tsai, "Suppressing CSR microbunching in recirculation arcs", in *Proc. 9th Int. Particle Accelerator Conf. (IPAC'18)*, Vancouver, Canada, Apr.-May 2018, pp. 1784–1789. doi:10.18429/JACoW-IPAC2018-WEYGBE1

[25] F. Zimmermann, "Estimates of CSR instability thresholds for various storage rings", CERN, Geneva, Switzerland, ATS-Note-2010-049, CLIC-Note-861, Dec. 2010.